https://doi.org/10.5194/egusphere-2026-4416
Preprint. Discussion started: 31 July 2026

Wildfire Hazard in Germany Under Worst-Case Conditions

Johannes Heisig[1] and Edzer Pebesma[1]

[1]Institute for Geoinformatics, University of Münster, Heisenbergstraße 2, 48149 Münster

Correspondence: Johannes Heisig (jheisig@uni-muenster.de)

Abstract.

Climate change is amplifying wildfire frequency and intensity in temperate Central Europe, making proactive hazard mapping essential for landscape mitigation. This study evaluates wildfire hazard in Germany under worst-case (i.e., near-maximum) environmental conditions to identify high-priority management zones. The minimum travel time algorithm was used to simulate over 50 million independent fires at a spatial resolution of 100 meters. The landscape was divided into seven distinct climatic fire occurrence areas and evaluated across all combinations of three wind speed percentiles (80th, 90th, and 97th) and three fuel moisture scenarios. We quantified hazard by integrating conditional burn probability (CBP) and conditional flame length (CFL). Fuel moisture emerged as the dominant driver of wildfire hazard, with drier conditions dramatically increasing simulated fire sizes and variances, whereas increases in wind speed had a negligible effect. Shrub fuels produced the most extreme fire behavior and frequently generated the longest flame lengths under worst-case conditions. Grass and forest fuels burned less intensely on average, but maximum aridity caused high-hazard forest areas to expand tenfold. Across the landscape, CBP remained highly skewed, revealing that a small number of volatile hotspots burn repeatedly while the vast majority of the country burns infrequently. The hazard map of Germany is dominated primarily by low hazard ratings, which cover large, continuous forest stands with dense overstorey canopies. Elevated hazards are concentrated in the northeast and west. These are represented either as an intensity-driven regime, defined by severe flame lengths, or a frequency-driven regime, characterized by a mix of fast-spreading grass and shrub fuels. The highest hazard ratings occur in open landscapes such as military areas and subalpine parklands, where rapid fire spread greatly increased burn probability. High-hazard zones consistently correlate with low canopy cover and reduced crown bulk density. This structural vulnerability is particularly evident in disturbed regions, where canopy dieback has simultaneously increased surface fuel loads and reduced the sheltering effect that typically dampens wind speeds and evaporation. Long-term wildfire mitigation in Germany should focus on high-hazard hotspots where volatile fuel configurations overlap with containment constraints resulting from terrain or unexploded ordnance. As fuels are the only landscape component that humans can actively manipulate, management frameworks must prioritize reducing understorey shrub loads, maintaining closed overstorey canopies, and diversifying forest structure, in order to build resilience against accelerating climate pressures.

https://doi.org/10.5194/egusphere-2026-4416
Preprint. Discussion started: 31 July 2026

1 Introduction

Climate change is increasing the frequency and duration of extreme fire weather, creating hazardous conditions in regions previously characterized by low fire activity (Miller et al., 2024). In European temperate forests the interplay of more frequent disturbances is altering the amount, composition, and moisture content of vegetation fuels, amplifying wildfire hazard and risk (Seidl et al., 2017). The 2022 wildfire season demonstrated the drastic effects of this development with three wildfires in eastern Germany and in the border region with the Czech Republic burning approximately 1,000 ha each. These fires exhibited intense behavior with surface flame lengths of 2-3 meters, full crown fires and spotting (the aerial transport of embers that ignite new fires ahead of the main front) over several hundred meters (Expertenkommission Waldbrände Sommer 2022, 2023). A combination of factors caused fires to escape the initial response and complicated containment efforts: extreme heat and drought prior to and during the incidents, strong winds and gusts, large quantities of dead wood caused by bark beetle infestation, challenging terrain, and contamination with explosive ordnance. Situations like these reveal the urgent need for both short-term adaptation and long-term mitigation strategies (Bednar-Friedl et al., 2022). Wildfire modeling can guide the transition to a sustainable fire regime by identifying hazards and high-priority areas that require immediate management intervention (Leonardos et al., 2024).

In this context, it is important to distinguish between risk and hazard. According to the framework established by Scott et al. (2013), wildfire hazard is defined as a physical situation with the potential to cause damage to highly valued resources and assets, whereas risk reflects the expected loss. Although fire can have positive ecological impacts in fire-adapted ecosystems, the focus in temperate Central Europe remains on the destructive potential of wildfire. Quantifying hazard requires the integration of two independent components: conditional burn probability (CBP) and conditional flame length (CFL) (Scott et al., 2013). Hazard is only high when CBP, the likelihood of a fire reaching a specific location, and CFL, the potential fire intensity, are both high.

To provide actionable information for landscape-scale management, assessments typically simulate fire behavior at near-maximum fuel aridity and wind conditions. While the likelihood of such events occurring is low, a worst-case approach is essential for identifying the maximum potential wildfire behavior in a given area. This enables managers to recognize where fire intensity is likely to exceed specific suppression thresholds, thereby helping them to prioritize preventive options.

With this approach we want to assess wildfire hazard in Germany by answering three questions:

- (i) How do wind and fuel moisture affect wildfire hazard?
- (ii) Which surface and canopy fuels lead to high wildfire hazard?
- (iii) Which locations show an elevated wildfire hazard under worst-case conditions?

https://doi.org/10.5194/egusphere-2026-4416
Preprint. Discussion started: 31 July 2026

2 Data and methods

2.1 Fire landscape

The fire modeling landscape is composed of eight variables that describe vegetation fuels and terrain, which are outlined below. The dataset covers approximately 35.8 million ha of which 13.7 million ha (38.3%) are burnable. All input variables were resampled to a common raster grid with a spatial resolution of 100 meters and are summarized in Appendix A1.

2.1.1 Surface fuels

Surface fuel properties describe the complex arrangement of ground biomass particles with relevance to fire spread. In forest environments these include duff, litter, twigs, needles, leaves, downed woody debris, and live herbs or shrubs. Outside of forests, surface fuels may be dominated by (live or dead) grasses or shrubs. Key properties include load quantities for multiple diameter size classes (mass per area), surface area to volume ratio, fuelbed depth, and the moisture threshold of extinction. This characterization of the dead and live biomass provides the required inputs for the Rothermel (1972) fire spread equation. For simplicity several standard fire behavior fuel model systems encode representative sets of properties in a categorical variable to define a manageable number of grass-, shrub-, and forest-dominated fuel models. The fuel models established by Scott and Burgan (2005) represent the fuel landscape of North America using 40 classes. Because Europe lacks such a system, many European fire modeling studies rely on the Scott & Burgan classification. Although standard fuel models are based on field measurements, their parameters are adjusted to ensure that their fire behavior estimates match reality.

Surface fuel properties are a critical factor in fire spread modeling as they determine the chance of an ignition and the horizontal and vertical propagation of the flame. The accuracy of surface fuel maps is therefore crucial to fire behavior estimates and the success of downstream hazard and risk assessments. At the same time surface fuels are more challenging to map than all other inputs of a fire spread model because of their high variability and the inability of remote sensors to penetrate overstorey vegetation (Keane et al., 2001). We used the recently published fuel model map product from Kutchartt et al. (2024), which has the highest spatial resolution (100 meters) out of all products available for our study area. Its level of spatial detail (1 ha) is sufficient to represent the typically small fires and forest patches in the fragmented landscapes of Germany. This product is derived from multiple land cover maps, climate data, and other remote sensing data, which come with their own errors and limitations. Besides concrete surfaces and water bodies, agricultural land is classified as *non-burnable* despite being flammable under extreme fire weather conditions. The goal of this study, however, is to assess hazard related to forest fires, as they involve much greater biomass volumes, energy release, and severity. To allow simulated fires to start on agricultural land and move into forested areas, we apply a 1-pixel buffer (100 meters) to forest edges that are adjacent to agricultural land. The buffered area is labeled as standard fuel model *GR3* (low-load, coarse, humid climate grass), which can produce low to medium flame length and rate of spread (Scott and Burgan, 2005). Figure 1 shows the frequency of each burnable fuel model in the study area and Appendix Table A2, respectively, lists the main parameters that affect fire behavior.

We tested how shrub (SH), timber-understorey (TU), and timber litter (TL) fuel models common to our study area behave under a range of wind and moisture conditions using the non-spatial fire behavior model *BehavePlus* (Andrews, 2007). Al-

https://doi.org/10.5194/egusphere-2026-4416
Preprint. Discussion started: 31 July 2026

though not assessing horizontal spread, it applies the same logic to vertical fire propagation as our spatial fire spread model. This approach is therefore suitable to approximate fire behavior across surface fuel types, identify thresholds for different types of fires, i.e., surface fire, and passive or active crown fire, and compare predicted and observed fire behavior. We modeled the ratio of fires that transition from a surface fire to a passive crown fire as a function of canopy base height, wind speed, and fuel moisture content. Beside the surface fuel model's burn properties, wind speed is the main driver of fire intensity and flame length. If the flame length surpasses a critical height threshold it reaches into the canopy, where it turns into a passive crown fire. There it may evolve into an active crown fire that moves through the canopy if crown bulk density and rate of spread exceed critical thresholds.

In settings with canopy base heights below 5 meters and low fuel moisture, shrub-dominated fuel models (*SH7* & *SH8*) only require very low wind speeds of 5-10 km/h to initiate a crown fire, whereas a base height of 9 meters leads to thresholds of 20-30 km/h. These value ranges are shifted by +5-10 km/h for two timber-understorey fuel models (*TU3* & *TU5*), while *TU2* only shows crown fire potential for extreme wind and moisture conditions. *TU1* and *TL3* are not capable of producing crown fire in any case. The wind speed thresholds for a transition to active crown fire depend on fuel moisture and range between 17 and 32 km/h. Consult Appendix Figure A1 for details.

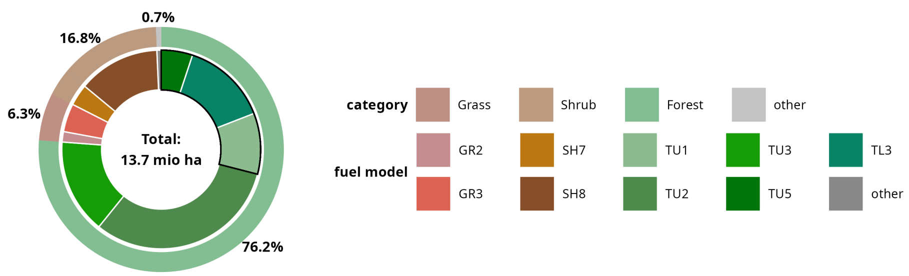

Figure 1. Relative frequencies of burnable fire behavior fuel model classes in the study area. Low-intensity forest fuel models *TU1* and *TL3* were assigned to *TU5*, indicated by the section outlined in black.

To facilitate the simulation of the extreme fire behavior including crown fire we edited the surface fuel model data by converting *TU1* and *TL3* to *TU5*. Pixels with land cover or land use type *concrete*, *water*, or *irrigated agriculture* were labeled as non-burnable which leaves them unaffected by a simulated fire and lets them act as a fire barrier. With a pixel size of 100 meters the fuel model map has the coarsest spatial resolution of all map inputs and therefore determines the pixel size of all fire spread simulation outputs.

2.1.2 Canopy fuels

The forest canopy is characterized by four variables: (i) top height; (ii) base height, as the lowest living branch of the crown; (iii) cover, as the percentage of the ground that is vertically shaded by the canopy, and (iv) bulk density, as the mass of crown

https://doi.org/10.5194/egusphere-2026-4416
Preprint. Discussion started: 31 July 2026

foliage per volume. These properties affect fire behavior in multiple ways. Canopy cover influences air circulation and the amount of moisture and light available to live surface fuels. Height variables affect the potential of a surface fire transitioning into a more severe crown fire. Crown bulk density determines whether there is sufficient fuel to sustain and propagate the flame through the canopy. The canopy fuel inputs for this analysis stem from three sources. We used canopy height and base height from Heisig et al. (2025), where we predicted maps specifically for Germany and included 3D LiDAR, radar, multi-spectral, and biophysical features. Canopy cover information was obtained from the Copernicus Tree Cover Density product provided by the European Environment Agency (2024). The crown bulk density layer was adopted from Kutchartt et al. (2025) because it has the best available map prediction accuracy for dense forests (canopy cover >80%), which account for over 81% of the forests in the study area.

2.1.3 Terrain

Elevation, slope and aspect are important factors for the speed and direction of wind and fire spread, but also influence fuel moisture content through humidity or exposure to solar radiation. To provide terrain variables for the fire landscape we accessed the Copernicus Digital Elevation Model with 90-meter spatial resolution (European Space Agency and Airbus, 2022) and applied bilinear interpolation to match the fuel model raster grid. We used the *gdaldem* program (GDAL contributors, 2025) to derive slope and aspect rasters.

2.2 Fire occurrence areas

Burning conditions can vary significantly throughout our study area, which features, e.g., maritime versus continental influence, or alpine regions versus lowlands. To account for regional variability in climate, landscape, and fire occurrence and to ensure consistent fire spread results (Vogler et al., 2021), we established distinct geographic modeling areas, from here on referred to as fire occurrence areas (FOAs). We accessed 19 bio-climatic variables from the WorldClim dataset (Fick and Hijmans, 2017) at a spatial resolution of 30 arc seconds (~1km) using the *geodata* R-package (Hijmans, 2021). These variables describe climatic conditions based on the intra-annual variability of temperature and precipitation. Together with the terrain variables, they served as inputs to the Simple Linear Iterative Clustering (SLIC) algorithm implemented in the *supercells* R-package (Nowosad and Stepinski, 2022). Through an iterative process we found suitable values for parameters k (number of clusters) and *compactness*, yielding 7 FOAs (Figure 2). All FOA boundaries were buffered, creating a spatial overlap of 10 kilometers to allow fires to start outside the analysis area and prevent edge effects.

2.3 Wind and moisture scenarios

The two relevant weather variables for our analysis were wind speed and wind direction. We accessed hourly U- and V- wind components with a spatial resolution of 0.1° (~9 km) from the ERA5-Land dataset (Copernicus Climate Change Service, 2019). By choosing a temporal extent of 10 years (2014-2023) we balanced year-to-year variability and the effects of recent climatic changes in Central Europe. Wind vector components were spatially aggregated for each FOA and converted to 7

https://doi.org/10.5194/egusphere-2026-4416
Preprint. Discussion started: 31 July 2026

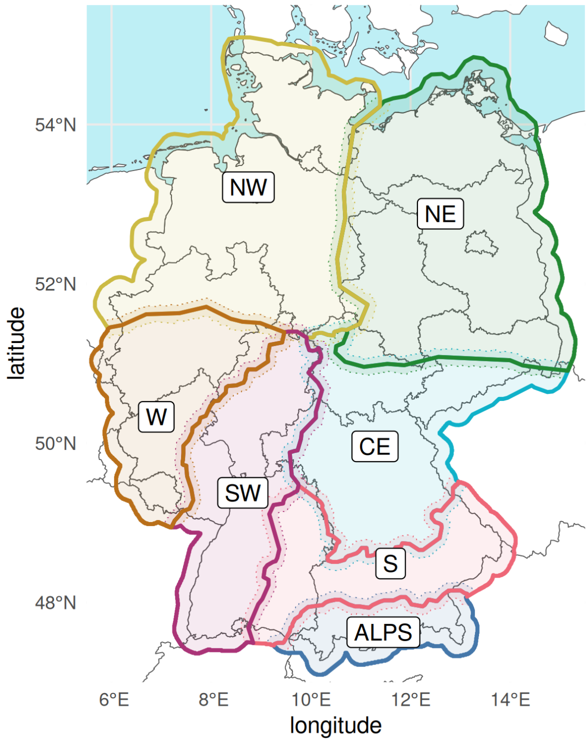

Figure 2. Fire occurrence areas (FOAs) define regions with homogeneous burning conditions. We created boundaries for 7 distinct FOAs by clustering bio-climatic variables: west (W), southwest (SW), northwest (NW), northeast (NE), center (CE), south (S), and the alpine region (ALPS).

corresponding hourly, one-dimensional time series of wind speed and wind direction. We calculated the 80th, 90th, and 97th percentile of the wind speed value distribution for each FOA to obtain three levels of high-fire-hazard wind conditions. We thereby include a near-maximum wind scenario and follow recommendations from similar work in the western United States (Scott et al., 2013).

Wind direction values were binned into four cardinal directions: east (45-135°N), south (135-225°N), west (225-315°N), and north (315-45°N). Each bin is represented by its center value (90°N, 180°N, 270°N, 0°N), which serves as the wind direction parameter in the fire spread model run. This approach is more appropriate than, e.g., only using the dominant wind direction, as it attempts to burn the landscape from all directions and avoids burn shadows in close proximity to non-burnable features. By maximizing the number of pixels burned we can derive more robust conclusions about the entire landscape. The relative wind direction frequency was computed for each bin and FOA to enable frequency weighting of the model outputs during post-processing (see Appendix Table A5 for details).

Fuel moisture content is another crucial parameter that heavily influences fire spread. It is closely linked to weather conditions and the availability of water and can be assessed for live and dead surface fuel components individually. To simulate a

https://doi.org/10.5194/egusphere-2026-4416
Preprint. Discussion started: 31 July 2026

range of wildfire conditions we selected three predefined moisture scenarios from a set proposed by Scott and Burgan (2005), namely D1L1, D2L2, and D3L3. These define the moisture content of three diameter size classes of dead (D) fuel particles (1-, 10-, and 100-hour fuels), as well as live (L) woody and herbaceous fuels. Higher digits indicate higher moisture content. By combining the three selected fuel moisture scenarios with three wind speed percentiles we obtain nine individual fire modeling scenarios (see Table 1) that reflect high to extreme fire hazard conditions. In this scenario grid, ’W’ denotes the wind speed component, and ’M’ denotes the moisture component. This selection of scenarios allows us to assess the potential impact of worst-case fires (scenario W1M1) and compare it to intense but less extreme cases.

Table 1. Fire modeling scenario grid constructed by combining 3 standard fuel moisture scenarios (M) with values for dead (D) and live (L) fuel components and 3 wind speed percentiles (W). Fire hazard is expected to be highest for W1M1 and lowest for W3M3. Wind speed values are computed from a 10-year time series for each of the 7 fire occurrence areas. For a detailed overview of wind speed and fuel moisture values see Appendix A4 and A5.

			Wind Speed Percentile		
			stronger	↔	*weaker*
			97	**90**	**80**
Fuel Moisture Scenario	*dryer*	**D1L1**	W1M1	W2M1	W3M1
	↕	**D2L2**	W1M2	W2M2	W3M2
	wetter	**D3L3**	W1M3	W2M3	W3M3

2.4 Fire spread simulation and hazard calculation

We simulated fire spread with *RandIG*, an efficient command-line version of the widely used *FlamMap* software (Finney, 2006). It is a deterministic modeling system that implements the minimum travel time (MTT) algorithm (Finney, 2002), which computes fire growth under environmental conditions that are constant over time (Finney, 2006). Following an ignition, the algorithm calculates fire intensity (flame length) depending on terrain, surface fuel properties, their moisture content, and wind speed. If canopy fuels are present and flame length exceeds a critical threshold, passive crown fire occurs. MTT further evaluates whether and how neighboring pixels begin to burn, which may be influenced by wind and spotting. If wind and crown fuels support fire propagation to neighboring pixels, passive fire may turn into an active, more devastating crown fire. Each simulation stops after a user-defined duration.

To find a suitable number of ignition locations we selected the ’least-burnable’ scenario (W3M3) and instructed *RandIG* to generate random ignitions until at least 95% of all burnable pixels have burned, which resulted in 5,696,288 ignitions. This way we assured the landscape is sufficiently burned in order to draw reliable conclusions when evaluating conditional burn probability and flame length. Selecting 95% as the target burn proportion is the result of an exploratory model run. Due to the fractured forest landscape in some parts of Germany there are many burnable but isolated pixels that can only start to burn through direct ignition, not through flame propagation from neighboring pixels. The benefit of burning the remaining (scattered

https://doi.org/10.5194/egusphere-2026-4416
Preprint. Discussion started: 31 July 2026

and often isolated) 5% of the landscape through random ignitions is outweighed by the increased computational cost. We used this exact set of ignition locations for all other scenario runs to ensure the comparability of results.

Static environmental conditions during each run are necessary for the same reason. However, *RandIG* uses the *WindNinja* model (Wagenbrenner et al., 2025) to generate gridded wind layers from static wind speed and direction values and terrain rasters. Allowing wind to vary in space based on terrain features makes the model's assumptions more realistic. We simulated fire spread for all combinations of FOAs (N=7), fire modeling scenarios (N=9), and wind directions (N=4) with a spatial resolution of 100 meters. In total over 50 million fires were simulated, each limited to a burn duration of 20 hours. The most relevant *RandIG* outputs for this study are conditional burn probability (CBP) and conditional flame length (CFL). CBP is calculated by dividing the number of times a pixel has burned by the total number of ignitions:

$$CBP = \frac{N_{burned}}{N_{ignitions}}$$

In this context it is important to note that CBP, like CFL, does not express the *actual* probability of a location burning but rather a probability that is *conditional* to a nearby ignition. CBP values need to be evaluated with respect to the maximum value of the respective scenario because they are sensitive to model parameters. To compare it across scenarios, we divide CBP by the maximum value of the respective scenario to create an independent index (CBP_i).

CFL estimates the average flame length weighted by the relative frequency that a pixel has burned at a certain fire intensity level (FIL; see Appendix Table A3). It is calculated as the sum-product of probabilities and mid-point flame lengths of all FILs

$$CFL = \sum_{i=1}^{n} FLP_i * FL_i$$

where FLP_i is the probability of FIL_i to occur and FL_i is the mid-point flame length representing FIL_i.

All modeling scenarios were simulated with wind coming from each of the four cardinal directions. We weighted CBP and CFL outputs according to the relative frequency of the respective wind direction for each FOA. The seven rasters were then mosaicked and overlapping pixel values were averaged. Both outputs were finally translated into categorical variables: CBP_i was binned into five equally sized intervals [0-0.2, ..., 0.8-1] and labeled from 'lowest' to 'highest'; CFL was assigned to its respective FIL.

We derived integrated wildfire hazard by combining CBP and CFL categories with a classification scheme provided by the Interagency Fuel Treatment Decision Support System (US Department of the Interior & US Department of Agriculture, 2026), visualized in Appendix Table A3. The system declares areas that show high CBP and CFL simultaneously as high fire hazard and vice versa. If only one of the two components is high, fire hazard remains medium to low. Non-burnable pixels (as per fuel model) and burnable, but not burned pixels are labeled as two additional classes. A secondary output of *RandIG* is the fire size list, which provides ignition locations and final fire sizes.

https://doi.org/10.5194/egusphere-2026-4416
Preprint. Discussion started: 31 July 2026

3 Results

Fuel moisture was found to be the most influential factor in this fire behavior simulation study. This becomes evident when comparing distribution curves of fire size related to different fuel moisture scenarios (Figure 3). Fires burning under the most flammable moisture scenario (D1L1) had a median size of 657 ha and exhibited greater variance than fires under wetter conditions. Scenarios with higher fuel moisture content, such as D2L2 and D3L3, led to median fire sizes of 328 and 166 ha, respectively. The increase in fire size with higher wind speed percentiles, however, was very limited.

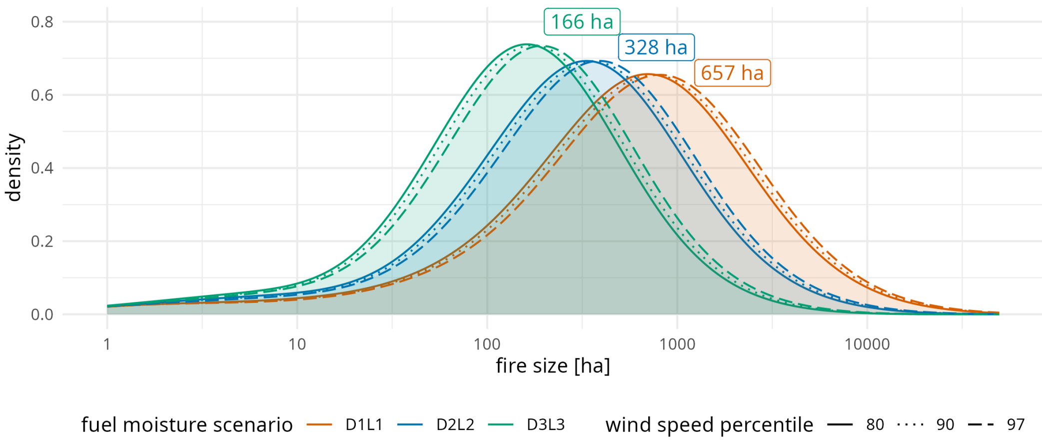

Figure 3. Distribution of fire sizes for all nine fuel moisture and wind speed scenario combinations (5,696,288 ignitions each). Curve labels present the median fire size by fuel moisture scenario. Fire size and variance (curve dispersion) grow with fuel aridity and wind speed. The effect of wind speed change is small compared to that of fuel moisture.

We observed similar patterns for wildfire hazard and its components (Figure 4). Increased fuel moisture, as expected, dampened fire spread, intensity, and therefore hazard. Extreme fire behavior under worst-case conditions was especially pronounced for shrub fuel models, as 75% (*SH7*) and 50% (*SH8*) of their respective area burned with a CFL taller than 2.4 meters. Grass and forest fuels burned less intense with the majority of their coverages in the 'lower' and 'lowest' hazard classes. In extreme conditions, however, they are capable of producing a CFL of 2 meters or more. 'Higher' and 'highest' wildfire hazard in forest areas (*TU2*, *TU3*, and *TU5*) accounted for 78,311 ha in scenario W1M3 compared to 827,908 ha in W1M1. This difference with a of factor 10 (∼0.6% vs ∼6% of the burnable area) again highlights the influence of moisture. Yet, it also reveals that a significant part of the German forest area is still highly flammable under less extreme conditions, given that the 30-year maximum of annual burned area is approximately 3,000 ha (Bundesanstalt für Landwirtschaft und Ernährung, 2022). CBP remained mostly low throughout all combinations of surface fuels and modeling scenarios. This distribution can be expected when few hot spots burn many times, while the vast majority of the landscape burns infrequently.

The primary application of this method is the identification of locations with high potential for destructive wildfires. Our hazard map (Figure 5) is dominated by estimates in the 'lower' and 'lowest' categories, which mainly cover large, contiguous

https://doi.org/10.5194/egusphere-2026-4416
Preprint. Discussion started: 31 July 2026

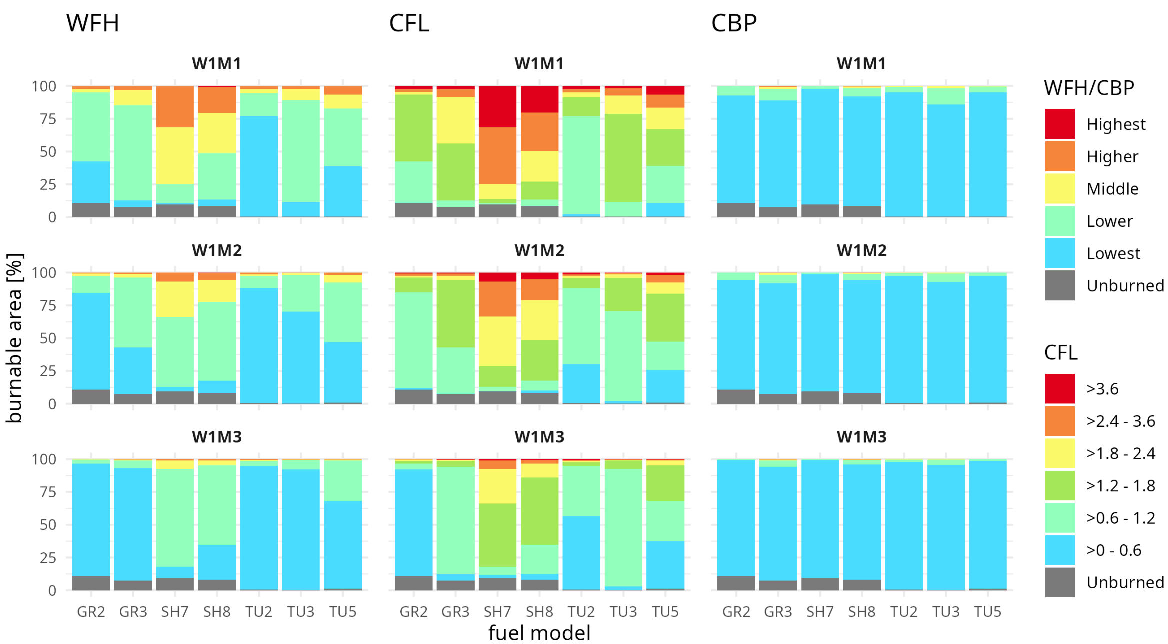

Figure 4. Relative distribution of wildfire hazard (WFH), conditional flame length (CFL; in meters), and conditional burn probability (CBP) categories among relevant surface fuel models (>1% of burnable area) for three fuel moisture scenarios. Shrub fuels show the highest frequency in high WFH and CFL with 20-30% in the flame length category above 3.6 meters (W1M1). Grass and forest fuels yield mainly low to medium WFH and CFL, with *TU5* leading to considerably larger fractions of higher or highest WFH than the rest ($\sim$ 7%, factor 2-3). Increased fuel moisture content (rows two and three) leads to similar, but attenuated frequency patterns. The lowest CBP category is constantly represented by over 80% of the burnable area, which can in part be explained by value scaling using the maximum CBP per run.

forests with tall and dense canopies. These are found in the central, southern, and northwestern FOAs. Medium to high hazard estimates generally occur in smaller quantities, but are more frequent in the western and northeastern FOAs, either clustered or along forest edges. In both cases shrub and grass fuels are adjacent to forest fuels, forming a heterogeneous landscape. This fuel configuration is highly susceptible to fire and common to the wildland-urban interface. In forests of northeastern Germany the more flammable *TU5* fuel model contributes to elevated fire hazard through high conditional flame length (Figure 5-i), defining an intensity-driven hazard regime. Vice versa, a more fragmented landscape and a larger proportion of grass and shrub fuels in western Germany lead to high conditional burn probability (Figure 5-iii), which describes a frequency-driven hazard regime.

Pixels classified as the 'highest' wildfire hazard category tend to appear in clusters scattered throughout the study area. The underlying landscape is dominated by grass- or heathland and surrounded by forest, which is a typical arrangement for military areas or subalpine parkland (Figure 5-iv). These large, contiguous patches of grass fuel produce high CBP values, as many fast-spreading fires overlap.

https://doi.org/10.5194/egusphere-2026-4416
Preprint. Discussion started: 31 July 2026

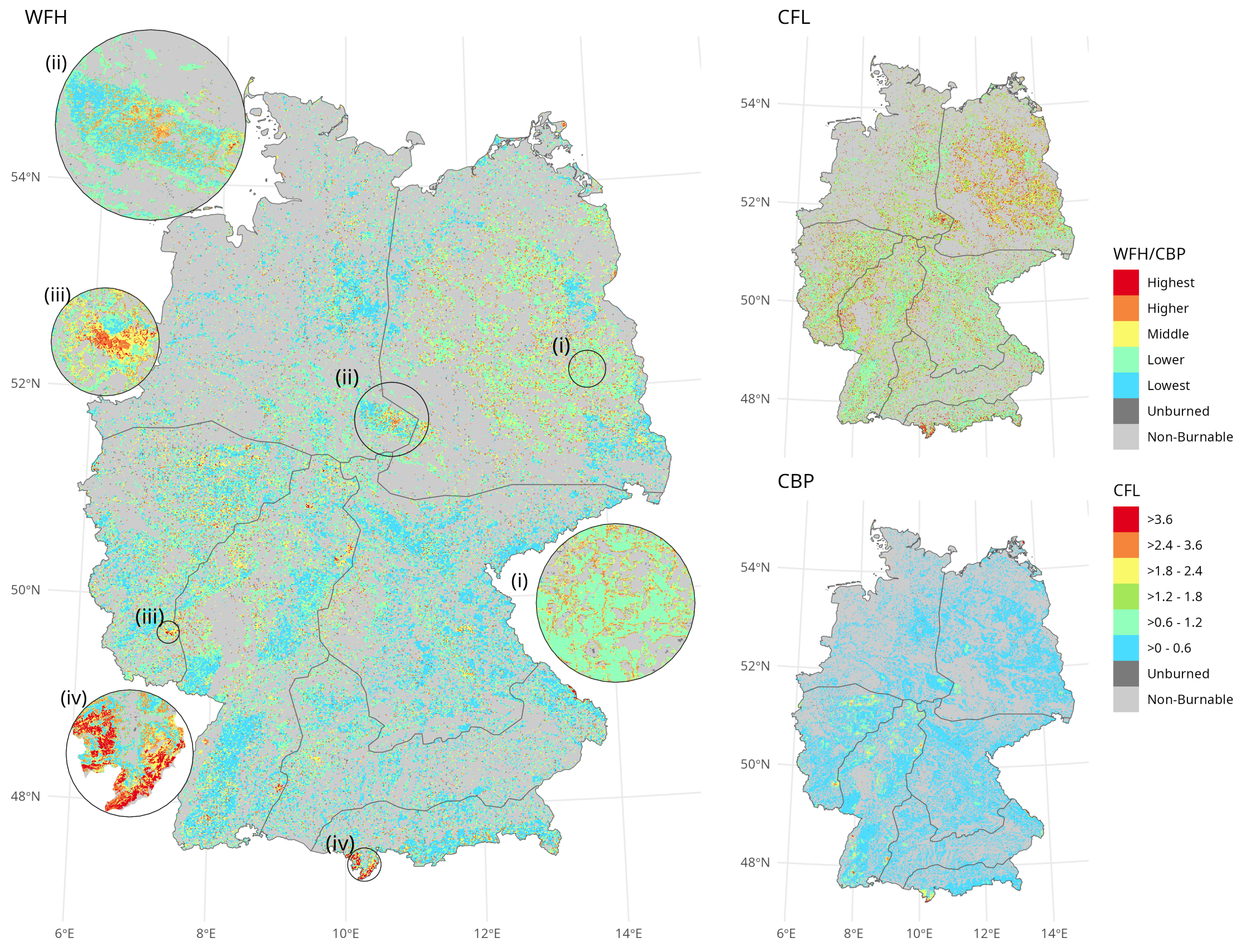

Figure 5. Maps of wildfire hazard (WFH), conditional flame length (CFL), and conditional burn probability (CBP) for Germany (scenario W1M1). The *TU5* fuel model drives CFL (and WFH) in the northeast through increased fire intensity (i). In the west, a more heterogeneous landscape of grass and shrub fuels interspersed with forests drives CBP (and WFH) through fast fire spread and large extents (ii). Clusters of high WFH occur in areas dominated by grass and shrub fuels with sparse or missing canopies, e.g., military areas (iii) or subalpine parkland (iv).

To gain more insight into the driving factors of high wildfire hazard ('higher' and 'highest' category) we compared the distribution of landscape variables for the entire landscape versus a subset of only high-hazard areas (Appendix Figure A2). Canopy fuel properties were generally lower for high-hazard areas across all surface fuel models. Larger differences were observed for canopy cover and crown bulk density in connection with forest fuels. Therefore, forest areas with sparser and lower crowns tend to be more susceptible to fire. An example for this setting can be observed in the Harz mountains (Figure 5-ii) where forest health has heavily declined in recent years (Thonfeld et al., 2022), leading to increased surface fuel loads and a reduced obstruction of wind or evaporation by the canopy.

https://doi.org/10.5194/egusphere-2026-4416
Preprint. Discussion started: 31 July 2026

4 Discussion

Surface fuels are the primary predictor of fire behavior. Their accurate quantification and their translation to modeling parameters that lead to realistic fire behavior estimates remain considerable challenges in fire science. Using standard fuel models as an abstract representation of fuels simplifies their characterization at the cost of introducing uncertainty from predictive modeling and obscuring fine-scale landscape variability. However, classifying fuel properties into standard fuel models remains common practice. Attempts to map individual fuel properties have been successful at a small scale using high-resolution 3D data. Yet, these methods are not (yet) feasible for large areas. This study relies on the Scott & Burgan fuel model system, which is specifically tailored to North American ecosystems and thereby introduces additional approximation error when applied in temperate Europe. The development of a standard surface fuel model set for (temperate) Europe is therefore urgently needed to facilitate more precise fire modeling.

After fuel loads, fuel moisture is the most influential component in the fire hazard equation. In reality, fuel moisture content varies over space and time due to its sensitivity to weather, soil, and microclimate conditions. The moisture scenarios used in this study, in contrast, greatly oversimplify this system. Similar to fuel loads, accurate remote sensing methods for the retrieval of moisture content of individual fuel components are being developed in local settings (Kranz et al., 2025), while reliable country- or continent-wide data is not available. We considered using a coarse dataset based on ERA5-Land, which provides live and dead fuel moisture content of wood and foliage biomass (McNorton and Di Giuseppe, 2024). The authors state that while it is currently the only dataset of its kind, it is based on multiple assumptions and its accuracy was only assessed indirectly due to a lack of global validation data. Because the data comes with an unknown error margin and fire spread is highly sensitive to dead fuel moisture content, we refrained from including it in this study. Our results support this decision by demonstrating considerable differences in, e.g., median fire size, resulting from changes in dead fuel moisture content of only 3% (compare Table A4). Instead we opted for a range of modeling scenarios that are appropriate for evaluating worst-case fire behavior to ensure comparability across space and scenarios at the same time. This approach entails a trade-off between comparability and applicability, as the likelihood of a certain scenario to occur varies by region.

Acknowledging these current limitations in fuel and moisture data for country-wide fire modeling, we implemented a probabilistic hazard framework that goes beyond deterministic fire behavior computation for single events. Instead we simulate millions of independent fires to receive statistically robust distributions for our target variables, reducing the impact of deficits in the input data. The robustness of our hazard maps could have been increased further by, e.g., raising the number of wind direction bins from 4 to 8 or more, or targeting a proportion of burned pixels larger than 95%. Both options would have greatly increased computational cost for little additional informative value, so they were omitted.

The wildfire hazard metric is derived as the product of two distinct categorical variables, where different combinations of flame length and burn probability classes can result in an identical hazard rating (compare Appendix Table A3). For this reason we can separate intensity-driven from frequency-driven regimes, which may have different requirements for future mitigation treatments.

https://doi.org/10.5194/egusphere-2026-4416
Preprint. Discussion started: 31 July 2026

Landscapes that are typical for the intensity-driven regime are characterized by high loads of large (100-hour) dead fuels (*TU5, SH7*) and sparse canopies, which allow the wind to reach the ground with substantial velocity. These factors create burning conditions in which the flame can consume sufficient biomass and oxygen, reach moderate to high lengths, and more easily transition to a high-intensity crown fire. This regime can be observed at the edges of northeastern pine forests. We expect our fuel data modification (adjoining grass fuels to forest edges) to have a promoting effect for fire hazard in these locations. Yet, this pattern is also plausible from an ecological perspective as forest edges have a more heterogeneous vertical structure, are more penetrable by wind, are exposed to more solar radiation, and can retain less moisture than dense forest interiors. Another example for high-intensity fire are clearings in degraded spruce stands like in the Harz Mountains, where the flame is carried by grass fuels and spreads to the more intensely burning shrub or forest fuels. In this case poor forest health and canopy dieback alter burning conditions including fuel load and wind speed and thereby increase wildfire hazard. We could improve our analysis by selecting a timber slash fuel model in areas that have large quantities of dead wood as a result of heavy disturbances, such as bark beetle attacks or windthrow.

In the frequency-driven regime, low to moderate loads of fine fuels (*GR3, TU3*) increase through dynamic curing. Live fuels with a high surface-area-to-volume ratio dry out quickly and a fraction of their load shifts to the 1-hour fuels, speeding up fire spread. This phenomenon is reinforced by high exposure to wind due to a sparse or missing canopy and sloped terrain that facilitates uphill winds and a preheating effect. Wildfire hazard under these conditions is mostly controlled by high burn probabilities rather than extreme flame lengths. Yet, if heavy-load shrub fuels (*SH8, SH9*) are present, flame length and hazard reach their highest categories. This is the case, for instance, in military training areas, where explosives frequently ignite fires and vegetation management is complicated by contamination. We also identified subalpine parklands above 1,000 meters as highly hazardous environments. These areas are traditionally considered to have a low probability of burning as the current climate at higher elevations makes extreme fire weather unlikely. In Austria, however, prolonged droughts were recently followed by mountainous forest fires that were difficult to contain due to the challenging terrain. As mountainous ecosystems are particularly vulnerable to climate change, these fires may soon become more common in Germany as well.

5 Conclusions

This study applied fire spread simulation to evaluate Germany's contemporary wildfire hazard under worst-case conditions, providing a baseline for nationwide fire management and climate adaptation planning. The results reveal that fuel moisture is the dominant driver of wildfire hazard, whereas shifting wind speed from high to extreme values only has minor effects on 2hazard ratings. Wildfire hazard is most severe where heavy-load shrub and forest surface fuels coincide with sparse overstorey canopies, while grass fuels accelerate horizontal spread.

Crucially, however, the majority of Germany's forest area shows low hazard potential even under extreme fire weather. This resilience is strongly maintained by healthy, continuous forest stands characterized by medium-to-high canopy cover. In contrast, proactive management should prioritize high-hazard hotspots such as forest edges, military areas, beetle-infested stands, and subalpine parklands. Mixed and contiguous fuel structures in these environments frequently overlap with serious

https://doi.org/10.5194/egusphere-2026-4416
Preprint. Discussion started: 31 July 2026

containment challenges, such as rugged terrain or unexploded ordnance contamination. Because fuel composition is the only component of the wildfire complex that humans can directly modify, long-term landscape resilience relies on targeted fuel management. This may include (i) the removal or reduction of heavy-load surface fuels, (ii) the transition toward greater species and structural diversity as a means of long-term adaptation to drought and fire, or (iii) the mitigation of fire in healthy stands through maintaining closed, high canopies and low surface fuel loads.

When combined with socio-environmental factors such as human ignition probability, our modeling outputs provide a valuable resource for the operational, country-wide mapping of wildfire risk with a high degree of spatial detail. Future research should build on this method by integrating more realistic fuel and moisture information as higher-resolution data becomes available, and by evaluating the efficacy of localized fuel treatment scenarios.

Code and data availability. The results of this study are available as 27 Cloud-Optimized GeoTiffs describing the three output variables and nine modeling scenarios at a 100-meter resolution. They can be downloaded from https://github.com/joheisig/Wildfire_Hazard_GER. The same repository contains a sample tile with all required inputs for one fire spread simulation run and corresponding outputs. It also stores code to run the entire analysis including pre- and postprocessing. However, the study can only be fully reproduced if one has access to the fire simulation software *RandIG*, which is not publicly available.

All output maps are additionally presented in an interactive web map that allows for a more detailed inspection of scenario-related differences and exact pixel values at high zoom levels: https://joheisig.github.io/Wildfire_Hazard_GER

Author contributions. JH: Conceptualization, data curation, formal analysis, investigation, methodology, project administration, resources, software, validation, visualization, writing – original draft, writing – review & editing. EP: Funding acquisition, supervision, writing – review & editing.

Competing interests. The authors declare no conflict of interest.

Acknowledgements. We would like to thank Dr. Faith Ann Heinsch and Gregory Dillon from the Missoula Fire Sciences Laboratory for their advice on fire modeling and fuel representation, as well as for granting us access to the *RandIG* fire modeling software. We would also like to thank Prof. Hanna Meyer and Dr. Jan Lehmann from the Institute for Landscape Ecology at the University of Münster for providing the compute infrastructure to run the simulation. DeepL Write was used to improve the text.

https://doi.org/10.5194/egusphere-2026-4416
Preprint. Discussion started: 31 July 2026

References

Andrews, P. L.: BehavePlus fire modeling system: past, present, and future, in: Proceedings of 7th Symposium on Fire and Forest Meteorology, p. 13, American Meteorological Society, Bar Harbor, ME and Boston, MA, 2007.

Bednar-Friedl, B., Biesbroek, R., Schmidt, D. N., Alexander, P., Børsheim, K. Y., Carnicer, J., Georgopoulou, E., Haasnoot, M., Le Cozannet, G., Lionello, P., Lipka, O., Möllmann, C., Muccione, V., Mustonen, T., Piepenburg, D., and Whitmarsh, L.: Europe, in: Climate Change 2022: Impacts, Adaptation and Vulnerability. Contribution of Working Group II to the Sixth Assessment Report of the Intergovernmental Panel on Climate Change, edited by Pörtner, H.-O., Roberts, D. C., Tignor, M., Poloczanska, E. S., Mintenbeck, K., Alegría, A., Craig, M., Langsdorf, S., Löschke, S., Möller, V., Okem, A., and Rama, B., pp. 1817–1927, Cambridge University Press, Cambridge, UK and New York, NY, USA, https://doi.org/10.1017/9781009325844.015, 2022.

Bundesanstalt für Landwirtschaft und Ernährung: Waldbrandstatistik der Bundesrepublik Deutschland für das Jahr 2022, Tech. rep., Bonn, Germany, https://www.bmel-statistik.de/fileadmin/daten/0302250-2022.pdf, 2022.

Copernicus Climate Change Service: ERA5-Land hourly data from 1950 to present, https://doi.org/10.24381/CDS.E2161BAC, 2019.

European Environment Agency: Tree Cover Density 2018 - Present (raster 10m), Europe, yearly, https://doi.org/10.2909/E677441E-FB94-431C-B4F9-304F10E4DFD8, 2024.

European Space Agency and Airbus: Copernicus DEM, https://doi.org/10.5270/ESA-c5d3d65, 2022.

Expertenkommission Waldbrände Sommer 2022: Bericht der Expertenkommission Waldbrände Sommer 2022 in Sachsen, Abschlussbericht, Sächsische Staatskanzlei, Dresden, https://www.staatskanzlei.sachsen.de/bericht-expertenkommission-waldbraende-sommer-2022, 2023.

Fick, S. E. and Hijmans, R. J.: WorldClim 2: new 1-km spatial resolution climate surfaces for global land areas, International Journal of Climatology, 37, 4302–4315, https://doi.org/10.1002/joc.5086, 2017.

Finney, M. A.: Fire growth using minimum travel time methods, Canadian Journal of Forest Research, 32, 1420–1424, https://doi.org/10.1139/x02-068, 2002.

Finney, M. A.: An overview of FlamMap fire modeling capabilities, in: Proceedings RMRS-P-41, vol. 41, pp. 213–220, Andrews, Patricia L.; Butler, Bret W., Fort Collins, CO, uS Department of Agriculture, Forest Service, Rocky Mountain Research Station, 2006.

GDAL contributors: Geospatial Data Abstraction software Library, https://doi.org/10.5281/zenodo.5884351, 2025.

Heisig, J., Milenković, M., and Pebesma, E.: High-resolution canopy fuel maps based on GEDI: a foundation for wildfire modeling in Germany, Environmental Research: Ecology, 4, 015 003, https://doi.org/10.1088/2752-664X/adaaf9, 2025.

Hijmans, R. J.: geodata: Access Geographic Data, https://doi.org/10.32614/CRAN.package.geodata, institution: Comprehensive R Archive Network Pages: 0.6-6, 2021.

Keane, R. E., Burgan, R., and van Wagtendonk, J.: Mapping wildland fuels for fire management across multiple scales: Integrating remote sensing, GIS, and biophysical modeling, International Journal of Wildland Fire, 10, 301, https://doi.org/10.1071/WF01028, number: 4, 2001.

Kranz, J., Bauer, K., Pampanoni, V., Zhao, L., Marrs, C., Mauder, M., Poděbradská, M., Van Der Maaten-Theunissen, M., Yebra, M., and Forkel, M.: Assessing predictors for fuel moisture content in Central European forests, Agricultural and Forest Meteorology, 371, 110 590, https://doi.org/10.1016/j.agrformet.2025.110590, 2025.

Kutchartt, E., González-Olabarria, J. R., Aquilué, N., Garcia-Gonzalo, J., Trasobares, A., Botequim, B., Hauglin, M., Palaiologou, P., Vassilev, V., Cardil, A., Navarrete, M. , Orazio, C., and Pirotti, F.: Pan-European fuel map server: An open-geodata portal for supporting fire risk assessment, Geomatica, 76, https://doi.org/10.1016/j.geomat.2024.100036, 2024.

Kutchartt, E., González-Olabarria, J. R., Trasobares, A., Aquilué, N., Guerra-Hernández, J., Nunes, L., Sequeira, A. C., Botequim, B., Hauglin, M., Palaiologou, P., Cardil, A., Rogai, M., Vassilev, V., Pimont, F., Martin-Ducup, O., and Pirotti, F.: Satellite-based mapping of canopy fuels at the pan-European scale, Geo-spatial Information Science, 28, 1465–1493, https://doi.org/10.1080/10095020.2024.2429376, 2025.

Leonardos, L., Gnilke, A., Sanders, T. G. M., Shatto, C., Stadelmann, C., Beierkuhnlein, C., and Jentsch, A.: Synthesis and Perspectives on Disturbance Interactions, and Forest Fire Risk and Fire Severity in Central Europe, Fire, 7, https://doi.org/10.3390/fire7120470, 2024.

McNorton, J. R. and Di Giuseppe, F.: A global fuel characteristic model and dataset for wildfire prediction, Biogeosciences, 21, 279–300, https://doi.org/10.5194/bg-21-279-2024, 2024.

Miller, J., Böhnisch, A., Ludwig, R., and Brunner, M. I.: Climate change impacts on regional fire weather in heterogeneous landscapes of central Europe, Natural Hazards and Earth System Sciences, 24, 411–428, https://doi.org/10.5194/nhess-24-411-2024, 2024.

Nowosad, J. and Stepinski, T. F.: Extended SLIC superpixels algorithm for applications to non-imagery geospatial rasters, International Journal of Applied Earth Observation and Geoinformation, 112, https://doi.org/10.1016/j.jag.2022.102935, 2022.

Rothermel, R. C.: A mathematical model for predicting fire spread in wildland fuels. USDA Forest Service, Research Paper INT-115, Ogden, Utah, USA, 40., Tech. rep., 1972.

Scott, J. H. and Burgan, R. E.: Standard fire behavior fuel models: a comprehensive set for use with Rothermel's surface fire spread model, Tech. Rep. RMRS-GTR-153, U.S. Department of Agriculture, Forest Service, Rocky Mountain Research Station, Ft. Collins, CO, https://doi.org/10.2737/RMRS-GTR-153, issue: RMRS-GTR-153, 2005.

Scott, J. H., Thompson, M. P., and Calkin, D. E.: A wildfire risk assessment framework for land and resource management, Tech. Rep. RMRS-GTR-315, U.S. Department of Agriculture, Forest Service, Rocky Mountain Research Station, Ft. Collins, CO, https://doi.org/10.2737/RMRS-GTR-315, 2013.

Seidl, R., Thom, D., Kautz, M., Martin-Benito, D., Peltoniemi, M., Vacchiano, G., Wild, J., Ascoli, D., Petr, M., Honkaniemi, J., Lexer, M. J., Trotsiuk, V., Mairota, P., Svoboda, M., Fabrika, M., Nagel, T. A., and Reyer, C. P. O.: Forest disturbances under climate change, Nature Climate Change, 7, 395–402, https://doi.org/10.1038/nclimate3303, 2017.

Thonfeld, F., Gessner, U., Holzwarth, S., Kriese, J., da Ponte, E., Huth, J., and Kuenzer, C.: A First Assessment of Canopy Cover Loss in Germany's Forests after the 2018–2020 Drought Years, Remote Sensing, 14, 562, https://doi.org/10.3390/rs14030562, number: 3, 2022.

US Department of the Interior & US Department of Agriculture: Interagency Fuels Treatment Decision Support System (IFTDSS) (version 3.11), https://doi.org/https://iftdss.firenet.gov/, 2026.

Vogler, K. C., Brough, A., Moran, C. J., Scott, J. H., and Gilbertson-Day, J. W.: Contemporary Wildfire Hazard Across California, Tech. rep., http://pyrologix.com/reports/Contemporary-Wildfire-Hazard-Across-California.pdf, 2021.

Wagenbrenner, N., Shannon, K., latwood, tfinney9, masonwillman, Forthofer, J., Kim, N., RuiyuZhang.SD, Gedlaman, H., Mehlitz, P. C., lmnn3, Brittain, S., greynathan, MelonDeLaMancha, Marsh, C., Reddy, S., OfirGan, Wahbe, J., Díaz, H., Hayward, J., Kim, N., Dayani, G., jeffreycunn, and santiagoMonedero: WindNinja, https://doi.org/10.5281/zenodo.15604809, 2025.

https://doi.org/10.5194/egusphere-2026-4416
Preprint. Discussion started: 31 July 2026

Appendix A

Table A1. Input datasets for the fire landscape and wind scenarios and their native spatial resolution.

Category	Name	Native Resolution	Source
Landscape	Surface fuel map	100 m	Kutchartt et al. (2024)
	Canopy height & Canopy base height	20 m	Heisig et al. (2025)
	Tree cover density	10 m	European Environment Agency (2024)
	Crown bulk density	100 m	Kutchartt et al. (2025)
	Copernicus Digital Elevation Model (DEM)	90 m	European Space Agency and Airbus (2022)
	Slope / Aspect	90 m	Derived from Copernicus DEM
Weather	ERA5-Land U- / V- wind components	∼9000 m	Copernicus Climate Change Service (2019)
FOAs	WorldClim (19 variables)	∼1000 m	Fick and Hijmans (2017)

Table A2. Selection of standard surface fuel models from Scott and Burgan (2005) common to our study area and parameters relevant to fire behavior.

Code	Group	Fuel load (t/ha)					Fuel bed depth (m)	Dead fuel extinction moisture (%)
		Dead			Live			
		1-hr	10-hr	100-hr	herb	woody		
GR2	Grass	0.2	0.0	0.0	2.2	0.0	0.3	15
GR3	Grass	0.2	0.9	0.0	3.4	0.0	0.6	30
SH7	Shrub	7.8	11.9	4.9	0.0	7.6	1.8	15
SH8	Shrub	4.6	7.6	1.9	0.0	9.7	0.9	40
TU1	Timber-Understory	0.5	2.0	3.4	0.5	2.0	0.2	20
TU2	Timber-Understory	2.1	4.0	2.8	0.0	0.5	0.3	30
TU3	Timber-Understory	4.1	0.3	0.6	1.5	4.1	0.4	30
TU5	Timber-Understory	9.0	9.0	6.7	0.0	6.7	0.3	25
TL3	Timber Litter	1.1	4.9	6.3	0.0	0.0	0.1	20

https://doi.org/10.5194/egusphere-2026-4416
Preprint. Discussion started: 31 July 2026

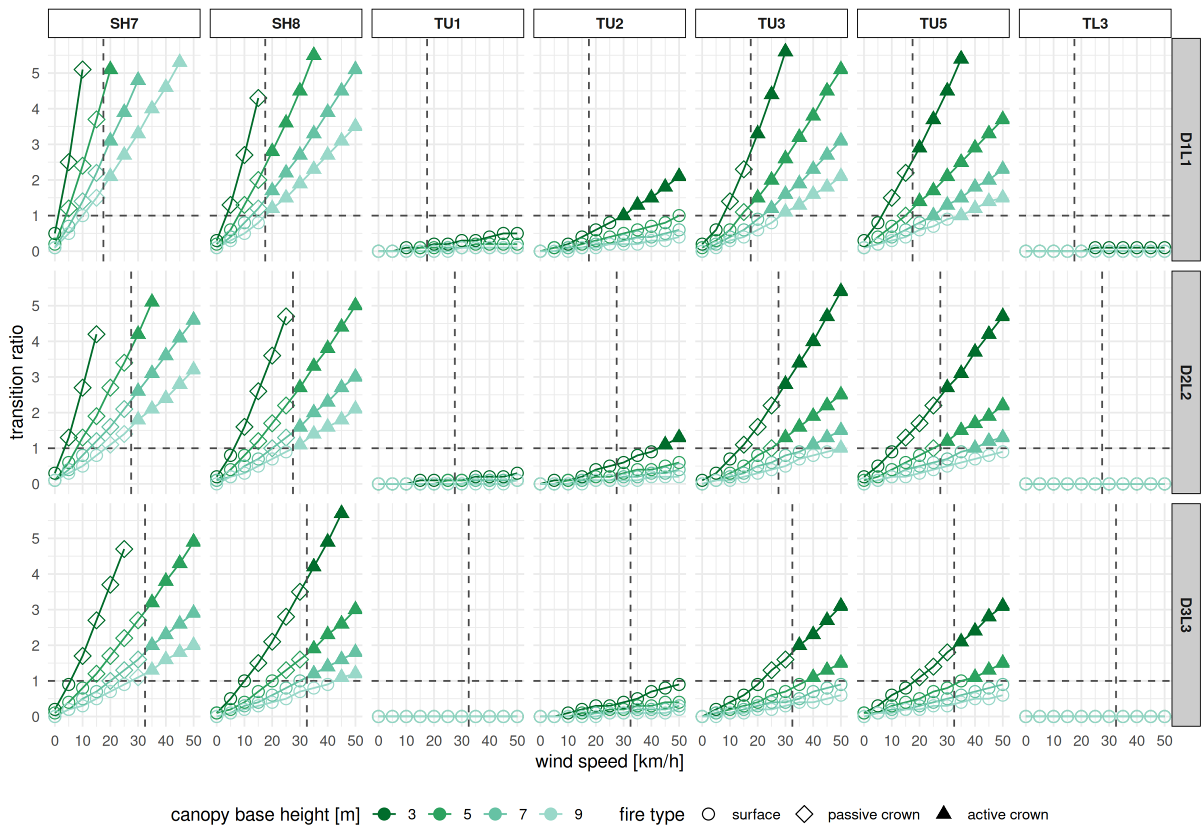

Figure A1. Transition (from surface to crown fire) ratio plotted against wind speed for common shrub (SH), timber-understorey (TU), and timber litter (TL) fuel models (Scott and Burgan, 2005) in the study area (columns), three fuel moisture scenarios (rows; see Appendix Table A4), and a range of canopy base heights (darker color shading indicates lower overstorey). A transition ratio of 1 (dashed horizontal line) marks the threshold of a surface fire (points) reaching into the canopy to become a passive crown fire (diamonds). When passing the (wind-driven) fire intensity threshold (dashed vertical line), passive can turn into an active crown fire (triangles). Fuel models *TU1* and *TL3* are not capable of producing crown fire. *TU2* may technically show active crown fire for very high wind speeds and very low fuel moisture, but only if low canopy is present. Only *SH7/8* and *TU3/5* can induce significant fire behavior at low to moderate wind speeds.

https://doi.org/10.5194/egusphere-2026-4416
Preprint. Discussion started: 31 July 2026

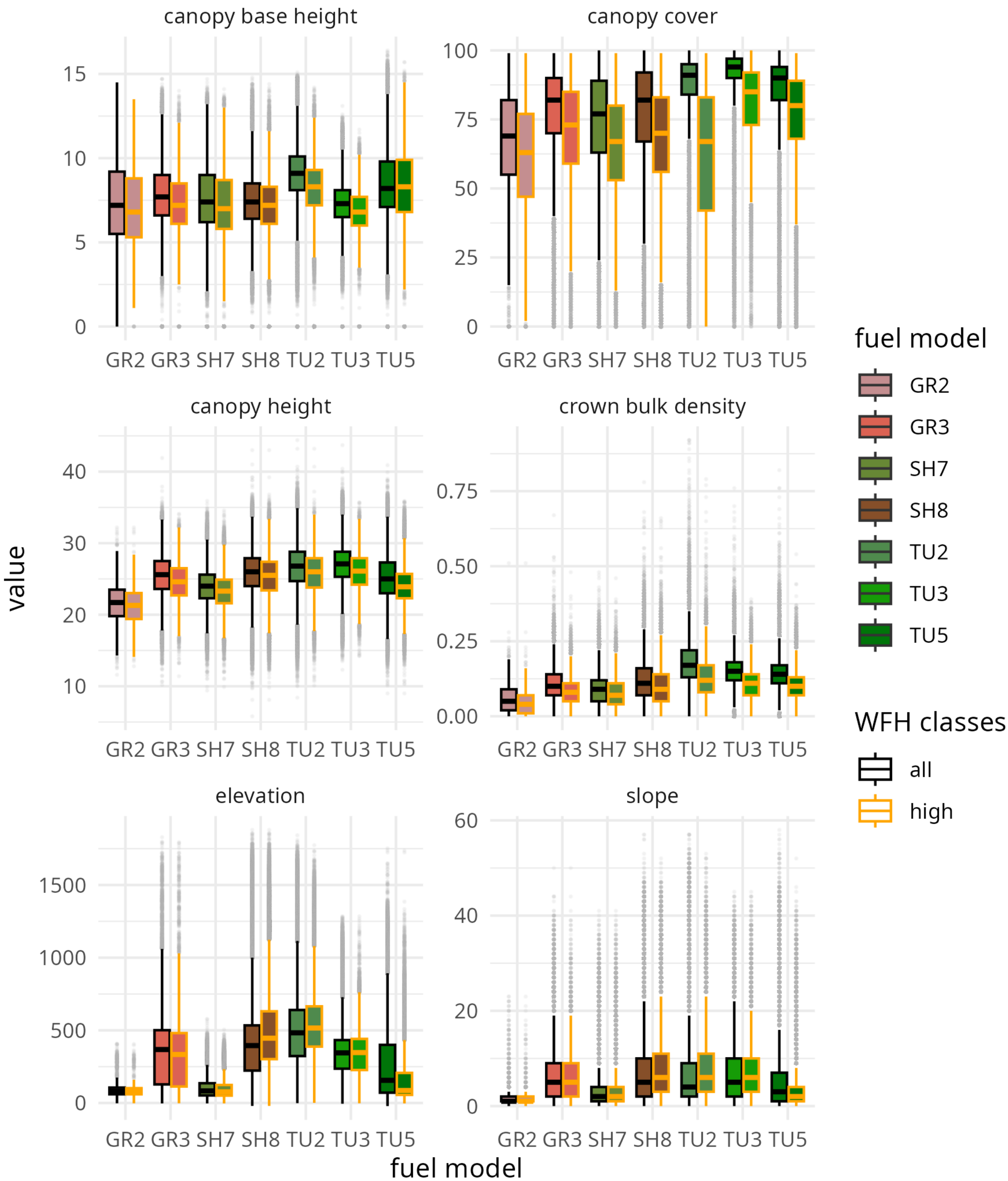

Figure A2. Boxplots of landscape variables across relevant surface fuel models (>1% burnable area) for all pixels (black boxes) and filtered for pixels with high wildfire hazard values ('higher' and 'highest'; orange boxes). On average, canopy fuel metrics are lower in areas with high hazard potential. For forest fuel models this difference is most pronounced in canopy cover and crown bulk density. For fuel models *SH8*, *TU2*, and *TU3*, fire hazard tends to increase with elevation and slope.

https://doi.org/10.5194/egusphere-2026-4416
Preprint. Discussion started: 31 July 2026

Table A3. Integrated wildfire hazard classification scheme for combining conditional burn probability (CBP) and conditional flame length (CFL) categories. CBP is scaled to a range of 0-100% using the absolute maximum value of the respective scenario and classified into five equal bins. CFL values are binned into predefined fire intensity levels (FILs), each represented by a mid-point flame length. High fire hazard is expected in areas with high CBP and high CFL simultaneously. Adapted from US Department of the Interior & US Department of Agriculture (2026).

Classes			**Conditional Burn Probability**				
			Lowest	**Lower**	**Middle**	**Higher**	**Highest**
	FIL	**mid-point FL**	0-20%	20-40%	40-60%	60-80%	80-100%
Conditional Flame Length	**>3.6 m**	7.6 m	Higher Hazard	Higher Hazard	Highest Hazard	Highest Hazard	Highest Hazard
	2.4-3.6 m	3 m	Middle Hazard	Middle Hazard	Higher Hazard	Higher Hazard	Highest Hazard
	1.8-2.4 m	2.1 m	Lower Hazard	Middle Hazard	Middle Hazard	Higher Hazard	Higher Hazard
	1.2-1.8 m	1.5 m	Lower Hazard	Lower Hazard	Middle Hazard	Middle Hazard	Higher Hazard
	0.6-1.2 m	0.9 m	Lowest Hazard	Lowest Hazard	Lower Hazard	Lower Hazard	Middle Hazard
	0-0.6 m	0.3 m	Lowest Hazard	Lowest Hazard	Lowest Hazard	Lower Hazard	Lower Hazard
Legend			**Lowest Hazard**	**Lower Hazard**	**Middle Hazard**	**Higher Hazard**	**Highest Hazard**

Table A4. Standard fuel moisture scenarios for surface fuels proposed by Scott and Burgan (2005), expressing fuel moisture content by surface fuel particle class in percent. Live and dead components can be combined individually, yielding 16 different scenarios. Our study uses scenarios D1L1, D2L2, and D3L3.

	Very low	Low	Moderate	High
Dead	**D1**	**D2**	**D3**	**D4**
1-hr	3	6	9	12
10-hr	4	7	10	13
100-hr	5	8	11	14
Live	**L1**	**L2**	**L3**	**L4**
Live herb	30	60	90	120
Live shrub	60	90	120	150

https://doi.org/10.5194/egusphere-2026-4416
Preprint. Discussion started: 31 July 2026

Table A5. Wind input values for *RandIG* model runs computed from a 10-year hourly time series (ERA5-Land; Copernicus Climate Change Service (2019)) for each fire occurrence area (FOA). Wind speed percentiles are used to construct fire modeling scenarios. Wind direction was classified using equally sized bins representing the four cardinal directions. Temporal relative frequencies guide the weighting of model outputs that are based on the respective wind direction.

FOA	**Wind Direction Temporal Relative Frequency**				**Wind Speed Percentile [km/h]**		
	N	**W**	**S**	**E**	**80**	**90**	**97**
ALPS	0.087	0.369	0.380	0.163	14	17	21
CE	0.154	0.420	0.230	0.196	19	21	26
NE	0.160	0.451	0.179	0.209	33	37	44
NW	0.197	0.448	0.176	0.179	36	40	48
S	0.089	0.454	0.202	0.255	17	20	24
SW	0.173	0.394	0.234	0.200	18	21	25
W	0.217	0.404	0.221	0.158	20	24	28